Inorganic Chemistry

Article

pubs.acs.org/IC

Covalent Grafting of Organic–Inorganic Polyoxometalates Hybrids onto Mesoporous SBA-15: A Key Step for New Anchored Homogeneous Catalysts

Richard Villanneau,*[†] Asma Marzouk,[‡] Yan Wang,[†] Aicha Ben Djamaa,[†,‡] Guillaume Laugel,[‡] Anna Proust,[†,§] and Franck Launay*[,‡]

[†]Institut Parisien de Chimie Moléculaire, UMR CNRS 7201, UPMC Univ Paris 06, 4 place Jussieu, Case 42, 75252, Paris Cedex 05, France

[‡]Laboratoire de Réactivité de Surface, UMR CNRS 7197, UPMC Univ Paris 06, site Le Raphael, 3 rue Galilée, Case 178, 94200 Ivry-sur-Seine, France

[§]Institut Universitaire de France, 103 Bd Saint-Michel, 75005 Paris, France

Supporting Information

ABSTRACT: Covalent grafting of heteropolyanions hybrids B,α-$[As^{III}W_9O_{33}\{P(O)(CH_2CH_2CO_2H)\}_2]^{5-}$ on 3-aminopropyl functionalized SBA-15 has been achieved through the formation of peptide bonds. The covalent link has been confirmed by using IR and ^{13}C CP MAS NMR spectroscopies. Electrostatic interactions between carboxylate and protonated amines have been discarded on the basis of the retention of POMs after repeated washings of the resulting material by ionic liquid (bmimCl). This is the first example of anchored monovacant polyoxometalates (POM) in which nucleophilic oxygen atoms are still available after incorporation into mesoporous supports. Further characterization of the textural properties of grafted materials has shown that they still retain an important mesoporosity, which is compatible with their potential use in heterogeneous catalysis. Such systems are thus interesting candidates for the preparation of anchored homogeneous catalysts in which the POMs would play the role of polydentate inorganic ligands for the active centers.

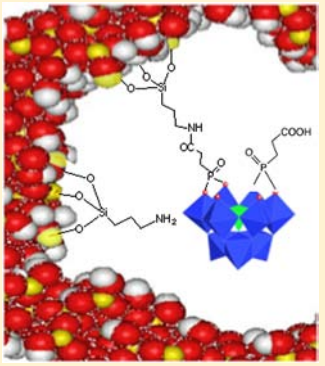

1. INTRODUCTION

Catalysis is considered as one of the pillars of green chemistry.[1] In particular in the field of oxidation reactions, there is a constant search for catalytic processes using dioxygen or hydrogen peroxide, i.e., "green" reagents that could substitute to noncatalytic technologies based on conventional oxidants (typically MnO_2, CrO_3, MnO_4^-, and so forth) affording stoichiometric amounts of nonvaluable byproducts. However, in the field of fine chemistry, alternative solutions are usually based on homogeneous metal-centered catalysts, and the principal limitations to their use are linked to separation problems, i.e., loss of (often expensive) active centers and contamination of the reaction products by metal traces that are incompatible with pharmacological applications. Heterogenization of soluble catalysts then constitutes an elegant solution, since it may lead to a stronger robustness and to a growing efficiency.[2] It may indeed allow the chemist to combine the activity and selectivity of the homogeneous catalyst with the ease of recovery of the heterogeneous one: "the best of both worlds".[3] However, the efficiency of the resulting materials is also linked to the optimization of both the dispersion and the accessibility of the active sites deposited on the support. One of the keys for obtaining such efficient materials is the use of anchoring platforms with high specific surface and porosity, such as oxides with structured mesopores.

Additionally, polyoxometalates (POMs), a particular class of transition-metal oxoanion nanosized clusters, and especially their metallic derivatives, have deserved general attention as oxidation catalysts.[4] Indeed, POMs are capable of acting as multidentate inorganic ligands with numerous advantageous properties: they are generally resistant to water and thermodynamically stable toward oxidation; they have an interesting tunability of redox and acid properties; they afford the stabilization of metallic cations with different oxidation states (for instance Ru in the range +II to + VI)[5] or coming from the entire periodic table of the elements.

The immobilization of POMs onto surfaces has been largely described in the literature. Most examples deal with nonvacant heteropolyacids that are bound to oxide supports through the protonation of hydroxyl groups of the surface and the interaction of the resulting $\equiv Si—OH_2^+$ species with external oxygen atoms of the POMs. These kinds of interactions, which require the utilization of heteropolyacids, limit actually the range of accessible POMs, since acidic salts are available for only a limited number of species regarding the whole literature. Some examples include the utilization of heteropolyacids as electrostatic linkers for the grafting of organometallic

Received: October 31, 2012
Published: February 26, 2013

   dx.doi.org/10.1021/ic302374v | Inorg. Chem. 2013, 52, 2958–2965

$\{Rh^{I}(COD)(P—P)\}^{+}$ hydrogenation catalysts onto an alumina support (COD = 1,5-cyclooctadiene; P—P are various diphosphine ligands, such as duphos or binap).[6] Anchoring procedures inside the channels of mesoporous materials or at the surface of oxide nanoparticles that have been functionalized with positive alkylammonium[7−15] or imidazolium[16−18] groups have been used more recently. These electrostatic interactions, even if they strengthen the POM−support link, do not however completely avoid the leaching of the supported active phase, in particular in the case of catalytic processes taking place in conventional polar solvents or a fortiori in ionic liquids.

A few examples have been described in which POMs can be covalently bound to an oxide support. This covalent linking is achieved following two kinds of approaches. In the first one, transition-metal substituted POMs are attached onto the surface via coordination of the transition-metal centers of the POM with nitrogen atoms of alkylamine-substituted porous materials. This approach has been used with $[M(H_2O)PW_{11}O_{39}]^{5-}$ ($M = Co^{II}$, Ni^{II}),[19−21] β-$[SiW_9O_{37}\{Co(H_2O)\}_3]$,[10−19] or $[Ln\{PW_{11}O_{39}\}_2]$.[11−22] However, lots of questions remain on the strength of the link between the transition cations and the surface during the catalytic process, with these cations playing also the role of the active centers. The second approach consists in the direct grafting of Keggin-type mono- or divacant POMs on the surface of ordered porous silica architecture via organosilane moieties.[23−25] In these last examples, POMs have been incorporated either by copolymerization of the POMs with silicon precursors or by a postsynthesis route. However, in both cases the authors used strategies in which the anchored POMs do not conserve coordinating sites.

In the present work, we propose to covalently anchor hybrid lacunary POMs (an organo-phosphonate derivative with formula B,α-$[As^{III}W_9O_{33}\{P(O)(CH_2CH_2CO_2H)\}_2]^{5-}$ onto a mesoporous support (an SBA-15 functionalized with propylamine groups) in order to improve the chemical linkage between both partners. We present here a new methodology based on the utilization of a bifunctional POM that contains useful organic functions for the covalent grafting onto a surface and nucleophilic oxygen atoms for the coordination of metallic cations at once.

2. EXPERIMENTAL SECTION

2.1. Materials. $Na_8H[B,\alpha\text{-}As^{III}W_9O_{33}]\cdot 24H_2O$ was prepared as described elsewhere.[26] 3-Phosphonopropanoic acid was obtained from Aldrich. Solvents and other reagents were obtained from commercial sources and used as received, except for triethylamine, which was distilled under low pressure before using.

IR spectra were recorded from KBr pellets on a Biorad FT 165 spectrometer. Raman spectra were recorded on solid samples on a Kaiser Optica Systems HL5R spectrometer equipped with a near-IR laser diode working at 785 nm. The ^{13}C-MAS and ^{31}P-MAS NMR experiments were performed on powdered samples at room temperature on a Bruker Avance 500 spectrometer (11.4 T) operating, respectively, at 125 MHz (^{13}C) and 202 MHz (^{31}P). The samples were spun at the magic angle at a frequency of 10 kHz in 4 mm-diameter rotors. In the case of ^{13}C-MAS NMR experiment, proton cross-polarization (CP-MAS) was applied with a contact time of 1.5 ms, and the recycle delay was 5 s. The ^{31}P-MAS spectra were obtained with proton CP. The following parameters were used: cross-polarization contact time, 2 ms, and recycle delay, 10 s. The ^{1}H (300.13 MHz), ^{13}C (75.6 MHz), and $\{^{1}H\}^{31}P$ NMR (121.5 MHz) solution spectra were recorded in 5 mm o.d. tubes on a Bruker Avance 300 spectrometer equipped with a QNP probehead. The ^{183}W spectra were recorded at 12.5 MHz on the Bruker Avance 300 spectrometer equipped with a triple-resonance low-frequency probehead with ^{31}P external decoupling coil for $\{^{31}P\}^{183}W$ NMR spectra. Chemical shifts are referenced with respect to external 85% H_3PO_4 (^{31}P), and to an external alkaline 2 M Na_2WO_4 aqueous solution (^{183}W), respectively, and were measured by the substitution method. For ^{183}W a saturated aqueous solution of the dodecatungstosilicic acid ($H_4SiW_{12}O_{40}$) was used as secondary standard ($\delta = -103.8$ ppm). Thermogravimetric analyses (TGA) were performed at air with a TA-Instrument SDT Q600. Elemental analyses were performed by the Service Central d'Analyse of the CNRS (Vernaison, France). N_2 sorption analyses were obtained at 77 K using an ASAP-2010 Micromeritics apparatus. Small-angle XRD measurements were carried out on a Bruker D8 Advance XRD diffractometer. X-ray fluorescence analyses were conducted with an energy dispersive spectrometer (XEPOS with Turboquant powder software).

2.2. Synthesis of the Hybrid POM (^{n}Bu$_4$N)$_3$NaH[As^{III}W$_9$O$_{33}${P(O)(CH$_2$CH$_2$CO$_2$H)}$_2$]: TBA$_3$NaH(1). $Na_8H[B,\alpha\text{-}As^{III}W_9O_{33}]\cdot 24H_2O$ (2.00 mmol, 5.75 g) was suspended into 50 mL of a solution of (^{n}Bu$_4$N)Br (8 mmol, 2.57 g) and 3-phosphonopropanoic acid (4.00 mmol, 0.62 g) in acetonitrile. Concentrated hydrochloric acid 37% (8 mmol, 0.66 mL) was added dropwise at room temperature. The resulting suspension was heated overnight at 83 °C, and then filtrated on a glass frit (no. 4). The solution was concentrated under vacuum to get a colorless oil. Ethanol and diethylether were successively added to the oil in order to remove the excess of phosphonopropanoic acid, and to recover the target compound as a white solid material. This compound can be recrystallized in hot DMF or acetonitrile (20 mL) (yield = 5.83 g, 89%). Anal. Calcd for $C_{54}H_{120}N_3Na_1As_1P_2W_9O_{39}$: C, 19.96; H, 3.72; N, 1.29; As, 2.31; Na, 0.71; P, 1.91; W, 50.91. Found: C, 20.20; H, 3.80; N, 1.41; As 1.90; Na, 0.63; P, 1.60; W, 51.10. ^{1}H NMR (CD_3COCD_3): δ (ppm) 2.18−2.30 (m, PCH_2CH$_2$COOH), 2.70−2.90 (m, PCH$_2$CH_2COOH). $^{13}C\{^{1}H\}$ NMR (CD_3SOCD_3): δ (ppm) 23.4 (d, $^{1}J_{P-C}$ = 134 Hz, 1C, PCH$_2$CH$_2$COOH); 28.0 (s, 1C, PCH$_2$CH$_2$COOH); and 174.3 (d, $^{3}J_{P-C}$ = 23 Hz, 1 C, PCH$_2$CH$_2$COOH). $\{^{1}H\}^{31}P$ NMR (CH_3CN/CD_3CN): δ (ppm) 29.0. ^{183}W NMR (CD_3SOCD_3): δ (ppm) −215.7 (s, 1W); −117.5 (d, $^{2}J_{P-W}$ = 11.8 Hz, 2W); −117.6 (d, $^{2}J_{P-W}$ = 10.1 Hz, 2W); −112.5 (s, 2W); −111.7 (s, 2W). IR (KBr, cm^{-1}): 3440(vs), 3200(m), 1725(m), 1662(m), 1202(m), 1178(m), 1025(m), 1005(m), 965(s), 905(s), 828(s), 778(vs), 663(w), 582(w), 514(m), 498(m). Raman (solid, cm^{-1}): 1127 (w), 1054 (w), 996 (m), 974 (s), 941 (m), 903 (m), 747 (m).

2.3. Synthesis of Anion B,α-[As^{III}W$_9$O$_{33}${P(O)(CH$_2$CH$_2$(CO)NHCH$_2$C$_6$H$_5$)}$_2$]$^{5-}$ (2). Coupling reaction of compound TBA$_3$NaH(1) with benzylamine. Complex TBA$_3$NaH(**1**) (0.65 g; 0.2 mmol) was introduced in a 100 mL Schlenk tube under argon and dissolved in 25 mL of freshly distilled acetonitrile. Triethylamine (0.17 mL; 1.12 g; 1.2 mmol) was then added and the mixture placed in an ice bath. Isobutylchloroformiate (0.16 g; 1.2 mmol) was then added, and the resulting solution was stirred for 30 min. The solution was allowed to reach room temperature, and benzylamine (0.26 g; 0.26 mL; 2.4 mmol) was finally introduced. The solution was stirred overnight at room temperature, checked by ^{31}P NMR spectroscopy (major peak at 26.3 ppm), and then centrifugated. The supernatant was removed, and the solvent was evaporated under vacuum, leading to the formation of a viscous oil. This oil was triturated with ethanol and diethylether until the formation of a precipitate. This solid was then dried overnight at 50 °C under vacuum. The solid has been analyzed by ^{31}P NMR spectroscopy, and we observed the persistence of some uncoupled carboxylate functions (≈5%). No chemical analysis was performed on this compound because of the presence of a noteworthy amount of triethylamine and of uncoupled functions.

Data for compound TBA$_x$Na$_y$(Et$_3$NH)$_z$ (**2**) follow. $^{13}C\{^{1}H\}$ NMR (CD_3SOCD_3): δ (ppm) ≈ 22.4 (d, $^{1}J_{P-C}$ ≈ 120 Hz, 1C, PCH$_2$CH$_2$CONH−);[27] 29.0 (s, 1C, PCH$_2$CH$_2$CONH−), 42.2 (s, 1C, NH−CH$_2$), 126.7 (s, 1C, C$_6$H$_5$−), 127.2 (s, 2C, C$_6$H$_5$−, 134.9), (s, 2C, C$_6$H$_5$−), 139.7 (s, 1C, C$_6$H$_5$−), and 171.7 (d, $^{3}J_{P-C}$ = 23 Hz, 1 C, {−CONH−}). IR (KBr, cm^{-1}): 3065 (w), 3025 (w), 1649 (m), 1535 (m), 1255 (m), 1167 (m), 1024 (w), 1002 (w), 962 (s), 905 (s), 825 (s), 775 (vs), 699 (m), 667(w), 580 (w), 514(m), 498(m).

dx.doi.org/10.1021/ic302374v | Inorg. Chem. 2013, 52, 2958−2965

2.4. Preparation of the Mesoporous SBA-15 Silica. Poly(ethylene oxide)-poly(propylene oxide)-poly(ethylene oxide) triblock copolymer of the EO_{20}-PO_{70}-EO_{20} type (Pluronic P123) (4.0 g) was added to 120 mL of distilled water and 20 mL of concentrated hydrochloric acid (37%). The mixture was heated at 40 °C until complete dissolution of Pluronic P123. TEOS was then added dropwise and the resulting suspension further heated at 40 °C for 24 h. A hydrothermal treatment was then performed at 100 °C in a FEP bottle for another 24 h duration. The suspension was filtered, and the obtained solid washed with water, dried at 60 °C, and finally calcined (24 °C/h) at 550 °C for 6 h.

2.5. Functionalization of SBA-15 Silica Using 3-Aminopropyltriethoxysilane (APTES). Preparation of two NH_2−SBA-15 samples follows. In a 100 mL round-bottom flask, 1.0 g of freshly dried SBA-15 silica (350 °C, 12 h) was added to 50 mL of anhydrous toluene. The flask was then placed in an ultrasound bath in order to obtain a better dispersion of the support in toluene. The resulting suspension was stirred at room temperature, and 2 mmol (0.5 mL) or 4 mmol (1.0 mL) of APTES was added. After 2 h, the reaction mixture was heated until toluene reflux and maintained at this temperature for 24 h. Then, the suspension was filtered. The recovered solid was washed successively by 15 mL of toluene, acetonitrile, and ethanol, and then dried in air. Finally, the solid was extracted using a Soxhlet during 24 h with dichloromethane as the solvent.

2.6. Covalent Binding of $TBA_3NaH(1)$ with NH_2-Functionalized SBA-15 Solids. Two materials (**A** and **B**) have been synthesized, starting from the two NH_2-functionalized SBA-15 samples with different amine loadings previously described:

Material **A**: Complex $TBA_3NaH(\mathbf{1})$ (0.65 g; 0.2 mmol) was introduced in a 100 mL Schlenk tube under argon and dissolved in 25 mL of freshly distilled acetonitrile. Triethylamine (84 μL; 0.06 g; 0.6 mmol) was then added and the mixture placed in an ice bath. Later, isobutylchloroformiate (78 μL; 0.08 g; 0.6 mmol) was introduced, and the resulting solution (solution 1) was stirred for 30 min. In parallel, 0.6 g of NH_2−SBA-15 sample with 2 mmol/g of $-NH_2$ groups (1.2 mmol) was dispersed in acetonitrile in another Schlenk tube under argon. Solution 1 was then transferred to the dispersion of the support using a cannula. The resulting suspension was stirred overnight at room temperature, and then filtered. The solid recovered was washed using ethanol and diethylether, dried, and finally extracted using a Soxhlet over 5 days with acetonitrile as the solvent.

Material **B** was prepared using a similar procedure starting from 0.6 g of NH_2−SBA-15 sample with 4 mmol/g of $-NH_2$ groups (2.4 mmol) using the following quantities of reagents: $TBA_3NaH(\mathbf{1})$ (0.65 g; 0.2 mmol), triethylamine (167 μL; 0.12 g; 1.2 mmol), and isobutylchloroformiate (156 μL; 0.16 g; 1.2 mmol).

3. RESULTS AND DISCUSSION

3.1. Choice of the Strategy for the Covalent Grafting. Silyl derivatives of POMs have been successfully used for the preparation of POMs-functionalized silicas.[23,25] In both cases, mesoporous materials with covalent links to α-$[SiW_{11}O_{39}\{O(SiOH)_2\}]^{4-}$ or γ-$[SiW_{10}O_{36}\{RSi\text{-}\mu\text{-}O\}_4]^{4-}$ moieties were obtained by copolymerization of TEOS or a mixture of TEOS and 1,2-bis(triethoxysilyl)ethane and the corresponding lacunary POMs. This methodology led to the formation of apparent regular mesoporous hybrid silicas, with POMs covalently linked on their walls. Moreover, the first system has shown a moderate catalytic activity for the epoxidation of cyclooctene with anhydrous H_2O_2 as a co-oxidant, which indicates a certain accessibility of the organic substrate to the POMs.[23] However in both cases the authors have pointed out some breaking of POMs/surface links, due to the relative weakness of the {Si−O−W} bonds, even after a moderate heating of the materials (45 °C).[25] Furthermore, due to the binding strategy implemented, no more nucleophilic oxygen atoms are available for metal substitution. Considering these two disadvantages inherent to such approaches, we turned ourselves to the use of trivacant Keggin-type polyanions bearing two alkylphosphonate groups with carboxylic terminal functions.

Indeed, bis-organophosphonate derivatives of the trivacant A,α-$[X^VW_9O_{34}]^{9-}$ (X = P, As) or B,α-$[X^{III}W_9O_{33}]^{9-}$ (X = As, Bi), respectively A,α-$[X^VW_9O_{34}\{RPO\}_2]^{5-}$ and B,α-$[X^{III}W_9O_{33}\{RPO\}_2]^{5-}$, are potentially bifunctional POMs: (1) They can be functionalized with R functions bearing several useful pending terminations, in the present case carboxylic acid functions. (2) More interestingly, only two phosphonate groups can be grafted onto the lacuna of the different trivacant anions, two over the six oxygen atoms that delimit the lacuna remaining insaturated.[28] Owing to this particularity they can then be used as ligands toward lanthanides or d transition metal cations.[29] We have reported on the coordination ability of A,α-$[P^VW_9O_{34}\{RPO\}_2]^{5-}$ anions, and we have recently extended this study to other platforms such as B,α-$[As^{III}W_9O_{33}\{RPO\}_2]^{5-}$.[29b]

These hybrids can be easily obtained at a 100 g scale in a single step, even in the case where R is a reactive pending group in refluxing acetonitrile or dimethylformamide and in the presence of aqueous concentrated HCl. Due to the robustness of {P−O−W} bonds compared to {Si−O−W} ones, these complexes are then really stable toward heating, hydrolysis, and acidic and moderately basic conditions.

However, the anchoring of such organophosphonyl-derivatives of POMs onto a surface is hardly achieved by co-condensation techniques, such as those developed in the case of organosilyl derivatives.[23−25] Even if reagents that contain terminal trisalkoxysilane and organo-phosphonyl ester groups at once do exist (for instance diethylphosphatoethyltriethoxysilane, PETES = $-(EtO)_3SiCH_2CH_2P(O)(OEt)_2$), it is impossible to control the specific grafting of the phosphonyl groups at the trivacant POMs. The presence in this case of a large excess of silyl functions during the reaction would undoubtedly lead to the saturation of the vacancy of the POM.

Owing to these difficulties but also to recent reports in the literature of homogeneous coupling reactions between hybrid POMs with various organic compounds,[31−36] we thus turned ourselves to a different pathway, which consists in the parallel preparation of functionalized POMs and silicas, with complementary organic functions (Scheme 1). These functions would finally react with each other in a second step. We thus prepared separately hybrid POMs and SBA-15 silica, the former bearing acid carboxylic groups, and the latter functionalized with primary amine functions.

Scheme 1. Representation of the Strategy Selected for Grafting a Hybrid POM onto a Functionalized Support

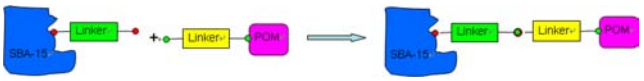

3.2. Preparation and Characterization of the Functionalized Mesoporous SBA-15. The functionalization of mesoporous silica by aminopropyl groups has been largely described due to the commercial availability of 3-aminopropyltriethoxysilane and the various applications of the resulting materials.[37,38] Grafting protocols usually differ by the solvent, expected loadings, and postsynthesis treatments. In this work, we have chosen to implement conditions gathering

dx.doi.org/10.1021/ic302374v | Inorg. Chem. 2013, 52, 2958−2965

the advantages of different published procedures. The SBA-15 silica support considered was prepared according to a conventional procedure.[39] It was characterized by a high hexagonal structuration of its mesoporosity (small-angle XRD, Figure S1) and textural parameters of good quality, i.e., S_{BET} (specific surface) = 985 ± 70 m^2 g^{-1}, Vp (pore volume) = 1.0 ± 0.1 cm^3 g^{-1}, and Dp (mean pore diameter) = 6.5 ± 0.2 nm. Among the important points, SBA-15 was preliminarily dried at 350 °C,[37] and functionalized materials were purified using Soxhlet extraction by dichloromethane. Otherwise, selected initial grafting conditions involve either 2 or 4 mmol of NH_2 groups per g of SBA-15 which is quite reasonable.[37]

Thermogravimetric profiles of NH_2−SBA-15 samples (Figure S2) are characterized by a first mass loss (about 3−4%) below 200 °C related to the departure of physisorbed molecules such as water and carbon dioxide and another one (11.5 and 23.1%) in the 200−900 °C range corresponding to the decomposition of 3-aminopropyl groups.[37,40] Estimated amounts of grafted functions are 2 and 4 mmol g^{-1} of silica, respectively, thus emphasizing the quantitative functionalization of the support in both samples. Introduction of aminopropyl groups is also demonstrated by infrared spectroscopy (Figure S3) through the appearance of new bands such as (1) υ(NH) at 3470 cm^{-1} that is partially masked by υ(OH) bands of silanol groups, (2) δ(NH) at ∼1540 cm^{-1},[41] and (3) υ(CH) bands of the propyl linker around 2938 cm^{-1}.

Functionalization also leads to modification of N_2 sorption isotherms (Figure S4) compared to those of SBA-15 precursor as a result of the decrease of the specific surface area, pore volume, and mean pore diameter. Such changes are consistent with the incorporation of at least part of the amino groups inside the mesopores.[42] Table 2 summarizes the textural characteristics of the silica SBA-15 before and after functionalization. It is found that 50% of the initial specific surface area is lost after the incorporation of 2 mmol of NH_2 g^{-1} whereas the reduction is about 60% with 4 mmol. Clearly, variation of the textural parameters is not proportional to the amount of amino groups introduced as a result probably of a worse dispersion in the highly loaded sample.

3.3. Preparation and Characterization of the Bis-carboxylate Derivative B,α-$[As^{III}W_9O_{33}\{P(O)(CH_2CH_2CO_2H)\}_2]^{5-}$ (1). The functionalization of various trivacant polyoxoanionic platforms with organo-phosphonic acids $RPO(OH)_2$ was previously described in our group.[28] This reaction is generally performed in acidic medium through the classical phase-transfer procedure using tetrabutylammonium cations as transfer agents.[30] We have already described the synthesis of A-type phosphotungstates with general formula A,α-$[PW_9O_{34}\{RPO\}_2]^{5-}$, and we report here on the preparation of the organo-phosphonate derivative with B-type, B,α-$[As^{III}W_9O_{33}\{P(O)(CH_2CH_2COOH)\}_2]^{5-}$ (**1**), using the same procedure. Due to the higher stability of B-type precursors compared to A-type, the formation of organophosphonate {P(O)R} derivatives where R is a very reactive function like $-CH_2CH_2COOH$ appears to be facilitated. Indeed, yields of $(^nBu_4N)_3Na_2[PW_9O_{34}\{P(O)(CH_2CH_2CO_2H)\}_2]$ hardly reached 40%, even in very polar solvents such as dimethylformamide.[29] Furthermore, whatever the conditions used, significant amounts of $(^nBu_4N)_3[PW_{12}O_{40}]$ were systematically formed. On the other hand, the preparation of pure $(^nBu_4N)_3NaH[As^{III}W_9O_{33}\{P(O)(CH_2CH_2CO_2H)\}_2]$ (compound TBA_3NaH(**1**), schematic representation of anion **1** in Figure 1) was easily performed in refluxing acetonitrile with yields close to 90%.

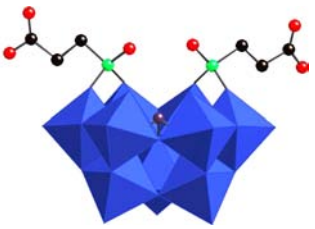

Figure 1. Polyhedral representation of the $[As^{III}W_9O_{33}\{P(O)(CH_2CH_2CO_2H)\}_2]^{5-}$ (**1**) anion. Oxygen atoms are represented in red, carbon in black, phosphorus in green, arsenic in mauve, and $\{WO_6\}$ octahedra in blue.

All these complexes, and in particular complex **1**, are characterized by the presence of four nucleophilic oxygen atoms (the two {RP═O} groups and the two unsaturated oxygen atoms delimiting the lacuna of the $\{XW_9\}$ anion) that are able to bind to metallic cations.[29]

Compound TBA_3NaH(**1**) was characterized by various spectroscopic methods (see SI for the details of the spectra). The ^{31}P NMR spectrum (Figure S5) displays a single peak at +29.0 ppm (in CD_3COCD_3) corresponding to the two equivalent phosphorus atoms from the {RPO} groups. The presence of a pair of satellites due to heteronuclear $^2J_{W-O-P}$ couplings confirms the grafting of these groups onto the $[AsW_9O_{33}]^{9-}$ core.

The ^1H spectrum of the compound shows the presence of 4 signals attributed to three tetrabutylammonium cations. Two multiplets assigned to the two different $-CH_2$ groups of the propionic acid chains are also observed in the range [2.18−2.30] and [2.70−2.90] ppm, respectively. They are however partially hidden by those of the tetrabutylammonium. We did not observe the signal of the −COOH groups. The presence of these functions has been proved by $\{^1H\}^{13}C$ NMR (Figure S6). Indeed, in addition to the four signals of the $^nBu_4N^+$ ions (13.5, 19.2, 23, and 57.5 ppm) and the two signals of the CH_2CH_2COOH chains (at 28.0 and 23.4 ppm), we observed a doublet centered at 174.3 ppm ($^3J_{P-C}$ = 23 Hz) assigned to the −COOH groups. The IR spectrum of TBA_3NaH(**1**) (Figure S7) displays several bands in the range [700−1000 cm^{-1}] characteristic of terminal W═O_t and bridging W−O_b−W bonds as expected for tungstates. In addition, we observed two bands at 1025 and 1005 cm^{-1}, assigned to the ν(As−O_c) and to the ν_{asym}(P═O) of the {RP═O} groups, respectively, by comparison with the phosphotungstate derivatives. The carboxylic acid function is evidenced by the presence of a $\nu_{C=O}$ band at 1725 cm^{-1} (close to that observed in free propionic acid) and of several small bands in the range 3000−3600 cm^{-1}, the strongest at 3440 cm^{-1} being assigned to pure ν_{OH}. Raman spectrum of TBA_3NaH(**1**) has also been recorded (Figure S11). Concerning the anion part, the strongest band is located at 974 cm^{-1}. The $\nu_{C=O}$ band, characteristic of the carboxylic function, is forbidden in Raman spectroscopy, and thus not observed.

TBA_3NaH(**1**) has been characterized by ^{183}W NMR spectroscopy. The $\{^{31}P\}^{183}W$ NMR spectrum displays four lines with relative intensity 2:2:4:1. This is compatible with the C_{2v} symmetry expected for anion **1**, provided that an accidental degeneracy of two lines is admitted. In order to confirm this statement, we have also recorded the ^{183}W NMR spectrum

dx.doi.org/10.1021/ic302374v | Inorg. Chem. 2013, 52, 2958−2965

(Figure 2). The spectrum displays five lines with relative intensity 2:2:2:2:1. However, two signals (those attributed to

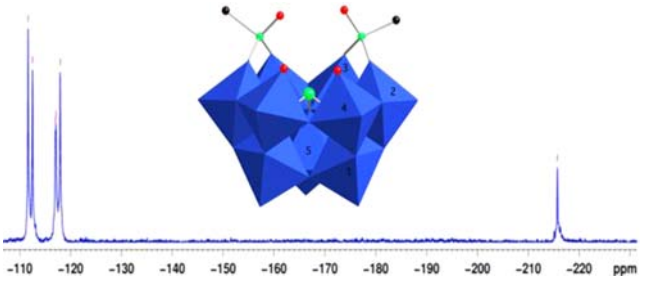

Figure 2. ^{183}W NMR spectrum of $TBA_3NaH(\mathbf{1})$.

W2 and W3, connected to the P atoms of the phosphonate groups, see Figure 2) are expected to be split. Providing that the signal at −117.1 ppm is in fact constituted of two components, we can thus deduce that the doublets attributed to W2 and W3 are (almost completely) overlapped and correspond to the lines at −117.1 and −118.0 ppm. The $^2J_{PW}$ coupling constants of each signal are consequently slightly different, and are, respectively, equal to 10.1 and 11.8 Hz, in good accordance with those observed for $[PW_9O_{34}\{P(O)R\}_2]^{5-}$.[28] The peak with lower relative intensity at −215.7 ppm is then attributed to W5 while the lines at −111.7 and −112.5 ppm may be assigned to the four other W atoms that are not connected to the phosphorus atoms (W1 and W4).

3.4. Postfunctionalization of B,α-$[As^{III}W_9O_{33}\{P(O)(CH_2CH_2CO_2H)\}_2]^{5-}$ (1). Prior to the grafting of anion **1** onto the amine functionalized support, the reactivity of its carboxylic acid functions in a coupling reaction with benzylamine has been studied. The second interest of this study was to provide spectroscopic data for the characterization of an amide function linked to the POM. The formation of peptide bonds using the carboxylic acids functions of **1** has been adapted from the method previously described by our research group in the case of organic/inorganic Wells−Dawson-type POM hybrids.[31] The optimized used procedure required the utilization of an activating agent (isobutylchloroformiate, ^{i}BuOC(O)Cl) in the presence of a base (NEt_3), in a ratio anion **1**/NEt_3/^{i}BuOC(O)Cl/benzylamine 1/6/6/12. The reaction has been monitored by ^{31}P NMR spectroscopy in acetonitrile. We observed the progressive decrease of the initial peak at 25.1 ppm[43] assigned to the carboxylate-containing phosphonate, and the appearance of a signal at 26.3 ppm, assigned to the amido-substituted phosphonate. After 16 h, the intensity of the carboxylate peak was less than 5% of the one assigned to the amide group. A solid has been isolated by evaporation of the solvent, washed with ethanol and diethylether, and characterized by IR and NMR spectroscopy.

The ^{31}P NMR spectrum (Figure S9) confirms the presence of a small amount of noncoupled functions in the solid. However, in the ^{13}C NMR spectrum (Figure S8), we did not observe the signal attributed to the carboxylate {C═O} functions due to their low amount. On the contrary, a new doublet is observed at lower field (δ = 171.7 ppm), as expected for an amide where the {C═O} is linked to N, i.e., a less electronegative atom than in a carboxylic acid function.

The IR spectrum is also instructive since we observed the disappearance of the $\nu_{C=O}$ band of the {COOH} group and the concomitant enlargement of the band at 1650 cm^{-1}, due to the δ_{OH} of residual water but also in this case to $\nu_{C=O}$ of an amide ("amide I band"). Furthermore, we observed two new bands at 1535 and 1255 cm^{-1} which can be attributed, respectively, to δ_{NH} ("amide II band") and ν_{CN} ("amide III band"). The presence of aromatic groups can be evidenced by two weak bands beyond 3000 cm^{-1} (3065 and 3025 cm^{-1}). The bands characteristic of the POM's core are essentially at the same position as in the spectrum of $TBA_3NaH(\mathbf{1})$, attesting to the conservation of the structure during the coupling reaction. All these data confirm that the new compound thus formed contains $[AsW_9O_{33}\{P(O)(CH_2CH_2CONHCH_2Ph)\}_2]^{5-}$ (anion **2**).

Despite careful washing of the solid with water, ethanol, and diethylether, we were not able to remove the contamination due to the initial presence of triethylamine. The latter has been evidenced by chemical analysis and ^{1}H NMR spectroscopy. This could indicate that some tetrabutylammonium has been exchanged with triethylammonium during the coupling reaction.

3.5. Covalent Grafting of the Polyoxometalates onto the SBA-15 Support and Characterization of the Resulting Material. Conditions used for the reaction of the bisphosphonopropanoic derivative of POM (anion **1**) with the NH_2-functionalized SBA-15 have been adapted from those established for the synthesis of anion **2**. In order to evaluate the effect of the loading of NH_2 groups on the POM uptake, two hybrid materials (**A** and **B**) have been prepared starting from the same amount (0.2 mmol) of the complex $TBA_3NaH(\mathbf{1})$ and 0.6 g of the NH_2-functionalized SBA-15 support with either 2 or 4 mmol of NH_2/g. Hence, the excesses of amine toward $-CO_2H$ groups in materials A and B were 3 and 6, respectively. In both experiments, the ratios between the coupling agent (^{i}BuOC(O)Cl), triethylamine, and the NH_2 functions were identical (1:1:2). POMs content in both materials has been checked by X-ray fluorescence spectroscopy (XRF). Surprisingly, the silica that contains fewer aminopropyl groups (2 mmol of NH_2/g) led to the incorporation of a higher amount of POM as shown in Table 1 (see This seems to indicate that

Table 1. XRF Analysis of SBA-15 Anchored Polyoxometalates

NH_2 content of the SBA (mmol/g)	W/Si[a] molar ratio	As/Si molar ratio	W/As molar ratio
2	0.08	7.2×10^{-3}	11.6
4	0.03	3.2×10^{-3}	11

[a]Expected values for W/Si, As/Si, and W/As are 0.23−0.25, 0.025−0.028, and 9. It is noteworthy that the ratio W/As obtained by XRF on pure $TBA_3NaH(\mathbf{1})$ was found equal to 11.3 instead of expected 9.

$-NH_2$ groups in highly loaded materials are less accessible to POMs, despite comparable textural properties of both NH_2-functionalized SBA-15 (respectively, 451 and 436 m^2 g^{-1}, see Table 2). This could be the result of a higher interpenetration of the organic chains at the surface of the mesopores at a concentration equal to 4.0 mmol of NH_2/g of support. It is noteworthy that best uptake of POM is almost one-third of the expected value. As expected, the greater amount of POM introduced (materials A), the greater the textural parameters are lowered. Even in the case of the higher incorporation ratio, mesopores with significant pore volumes are still available. The results presented below deal with material A because of its higher POM content.

dx.doi.org/10.1021/ic302374v | Inorg. Chem. 2013, 52, 2958−2965

Table 2. Textural Data of the Supports before and after Coupling

materials	S_{BET} (m^2 g^{-1})	pore volume (cm^3 g^{-1})	pore diameter (nm)
SBA-15	985	1.0	6.5
$-NH_2$ SBA-15 (2 mmol g^{-1})	451	0.6	5.9
A: POM@{$-NH_2$ SBA-15} (2 mmol g^{-1})	193	0.3	4.6
$-NH_2$ SBA-15 (4 mmol g^{-1})	436	0.5	5.7
B: POM@{$-NH_2$ SBA-15} (4 mmol g^{-1})	306	0.4	5.0

Demonstration for the retention of the integrity of POM entities upon grafting onto NH_2-functionalized SBA-15 was first brought by ^{31}P CP MAS of material A (inset in Figure 4) through the presence of a single large peak at 28 ppm. This one was observed in the same region as the signals obtained in solution for anions **1** and **2**, respectively. The superimposition of the Raman spectra (Figure S11) of pure $TBA_3NaH(\mathbf{1})$ and SBA-15 anchored anion **1** leads to the same conclusion. Indeed, the main bands observed on the spectrum of $TBA_3NaH(\mathbf{1})$ are also present on that of sample A. In particular, signals attributed to the $\nu_{(W=Ot)}$ and $\nu_{(W\text{-}Ob\text{-}W)}$ vibrations, in the range 700−1000 cm^{-1}, remain among the more intense in the Raman spectrum after the grafting step.

Evidences for Covalent Grafting of Polyoxometalates onto SBA-15. Evidence for the formation of amide bonds resulting from the reaction of the NH_2-functionalized SBA-15 with −COOH functions of anion **1** have been obtained using different physical techniques.

IR Spectroscopy. IR spectra of the NH_2-functionalized SBA-15 silica before and after reaction with $TBA_3NaH(\mathbf{1})$ are compared in Figure 3. Unlike Raman spectrum of the POM-

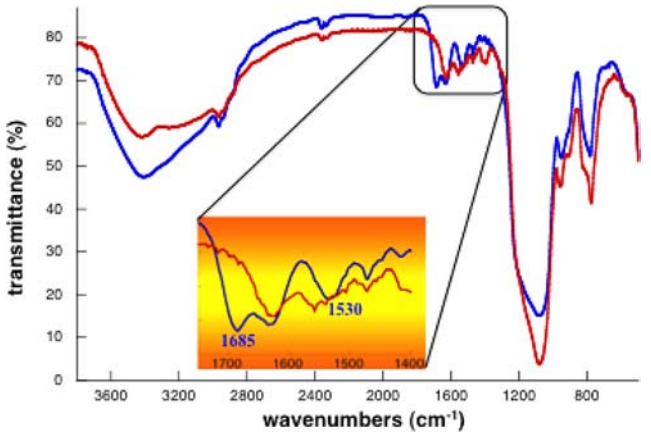

Figure 3. IR spectra of NH_2-functionalized SBA-15 with 2.0 mmol g^{-1} (in red) and of POM anchored onto SBA-15 support (in blue).

grafted materials, the polyoxometalate core may hardly be characterized by IR spectroscopy. Indeed, the presence of very intense bands in the range 800−1200 cm^{-1} attributed to the ν_{Si-O} vibrators strongly masks the characteristic bands of POMs in this region. Nevertheless, from Figure 3, one can notice an enhancement of a shoulder peak at 950 cm^{-1} that may be tentatively assigned to the $\nu_{(W=O)}$ band of the B,α-$[AsW_9O_{33}\{POR\}_2]^{5-}$ units. This technique is however more instructive regarding the nature of the (covalent) link between the POMs and the functionalized surface. Indeed, as observed for anion **2**, the spectrum of the POM-functionalized material displays new bands attributed to the amide function at 1685 and 1530 cm^{-1}, respectively, assigned to $\nu_{C=O}$ and δ_{NH} bands. Both bands are accompanied by the δ_{OH} one at 1636 cm^{-1}, also present in the NH_2-functionalized SBA-15 starting material.

^{13}C CP MAS NMR Spectroscopy. The presence of amide bonds in the final materials has been investigated also by ^{13}C CP MAS NMR spectroscopy. Figure 4 shows the spectrum of

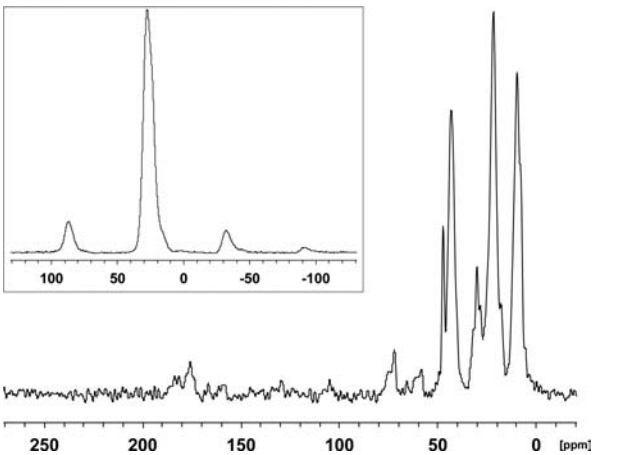

Figure 4. ^{13}C CP MAS NMR spectrum (inset: ^{31}P CP MAS NMR spectrum) of POM anchored onto SBA-15 support (material A obtained from NH_2-functionalized silica at 2.0 mmol of NH_2 g^{-1}).

the NH_2-functionalized SBA-15 silica after reaction with $TBA_3NaH(\mathbf{1})$. In the range 50−100 ppm, this spectrum displays predominantly the signals of the aliphatic carbon atoms from the aminopropyl groups of the surface and tetrabutylammonium cations. More interestingly, the two signals observed at 176 and 182 ppm, respectively, were assigned to carbon atoms of two different carbonyl functions. By comparison of the ^{13}C CP MAS NMR spectrum of the bis-amido derivative $TBA_xNa_y(Et_3NH)_z(\mathbf{2})$ (Figure S8, right) to that of $TBA_3NaH(\mathbf{1})$ simply deposited onto NH_2-functionalized SBA-15 (Figure S12), these signals were respectively attributed to the C atom of amide functions formed during the coupling reaction (176 ppm) and to the C atoms of residual carboxylic functions (182 ppm). These values are also in accordance with that expected for such functional groups in the literature. Such results confirmed that the covalent linking of anion **1** onto the NH_2-functionalized support was performed, and led us to propose that most of grafted POM **1** entities are linked through only one amide function, probably because the distance between the carboxylic functions does not match with the distribution of the NH_2 groups at the surface.

XRF Analysis of the Materials after a Washing Treatment with MeCN/Ionic Liquid Mixtures. Further proof for covalent attachment of POM (**1**) onto SBA-15 has been brought through the study of the leaching behavior of material A toward washing treatments with MeCN/N-butyl,*N*′-methylimidazolium chloride (e.g., bmimCl) mixtures for five days at 90 °C.

Hence, such an ionic and polar solvent mixture should lead to the dissolution of physically adsorbed POM-CO_2H species or favor the dissociation of possible $-NH_3^+\cdots{}^-O_2C-$POM surface ion pairs thus affording the solubilization of carboxylate form of compound **1**. For sake of comparison, two blank samples based on the impregnation of the functionalized support by a solution of $TBA_3NaH(\mathbf{1})$ in the presence (blank

dx.doi.org/10.1021/ic302374v | *Inorg. Chem.* 2013, 52, 2958−2965

with NEt_3) or in the absence of triethylamine (blank without NEt_3) were prepared using the same quantity of NH_2-functionalized SBA-15, POM, and triethylamine (when necessary) as for material A. All of these solids were treated similarly (washing in a Soxhlet in refluxing acetonitrile for 5 days, then by a solution of bmimCl for another 5 days).

The POM content of the recovered materials was analyzed by XRF spectroscopy before and after treatment with bmimCl (see Table 3). Whatever the protocol used, analysis results showed that POMs have been introduced in similar proportions in the three materials recovered. As expected, the decrease of POM loading after ionic liquid treatment was stronger for the two blank samples compared to material A, thus emphasizing a linkage that differs from simple physical adsorption or electrostatic interaction.

Table 3. XRF Analysis of POMs Anchored to SBA-15 (2.0 mmol.g^{-1}) before and after Washing with bmimCl/MeCN[a]

	atomic ratios			
	before washing with bmimCl		after washing with bmimCl	
materials	As/Si	W/Si	As/Si	W/Si
A: POMs@{$-NH_2$ SBA-15}	7.2×10^{-3}	0.08	4.8×10^{-3}	0.047
blank without NEt_3	7.0×10^{-3}	0.08	9.7×10^{-4}	0.011
blank with NEt_3	6.5×10^{-3}	0.07	1.9×10^{-3}	0.020

[a]Comparison with electrostatically or physically deposited POMs.

4. CONCLUSION

In this contribution, we have demonstrated, for the first time, that the functionalization of both vacant polyoxometalate species and mesoporous silica support by complementary organic functions provides an efficient strategy for their covalently linkage. The principle was illustrated using an organophosphonate derivative of trivacant POMs bearing carboxylic functionalities on one hand and an NH_2-functionalized mesoporous SBA-15 support on the other hand. In parallel, a similar molecular adduct has been prepared from the same organofunctionalized POM species and benzylamine to select optimal reaction conditions, and additionally to use its characterization patterns for a better demonstration of the preservation of the POM integrity and amide formation on the support. Integrity of the grafted POMs is important for further use as ligands. This was demonstrated by XRF, ^{31}P CP MAS NMR, and Raman spectroscopies. Strong association of the POMs through peptidic bond formation was evidenced by IR and ^{13}C CP MAS NMR spectroscopies. Exclusive physical adsorption or/and electrostatic interactions of $-NH_3^+\cdots{}^-O_2C-$ type were ruled out by putting in evidence the high resistance of hybrid materials toward MeCN/*N*-butyl,*N*′-methylimidazolium chloride, i.e., an ionic and polar solvent mixture well adapted for this purpose. Such a low leaching phenomena in organic medium and also ionic liquids as well as the confirmation of the persistence of mesopores in the materials despite the introduction of such large POM species make these solids interesting supports for heterogeneous catalysis. Further work on their reactivity is currently in progress.

■ ASSOCIATED CONTENT

Supporting Information

Structural characterization of compound TBA_3NaH(**1**) (^{13}C, ^{31}P NMR, IR spectroscopy) and of $TBA_xNa_y(Et_3NH)_z$(**2**) (^{13}C, ^{31}P NMR in solution or solid state); Raman spectra of pure TBA_3NaH(**1**) and of **1**-grafted onto NH_2-functionalized SBA 15 silica; structural (XRD), elemental (TGA), and textural (N_2 sorption) characterizations of SBA-15 NH_2 samples. This material is available free of charge via the Internet at http://pubs.acs.org.

■ AUTHOR INFORMATION

Corresponding Author

*E-mail: richard.villanneau@upmc.fr (R.V.).

Notes

The authors declare no competing financial interest.

■ ACKNOWLEDGMENTS

The authors want to thank Mrs. France Costa-Torro for help in ^{31}P and ^{13}C CP MAS NMR spectroscopy. This work was supported by the Centre National de la Recherche Scientifique (CNRS) and the Université Pierre et Marie Curie—Paris 6.

■ REFERENCES

(1) (a) Clark, J. H. *Green Chem.* **1999**, 1−8. (b) ten Brink, G.-J.; Arends, I. W. C. E.; Sheldon, R. A. *Science* **2000**, *287*, 1636−1639. (c) Sheldon, R. A. *Chem. Commun.* **2008**, 3352−3365.

(2) (a) Collman, J. P.; Hegedus, L. S.; Cooke, M. P.; Norton, J. R.; Dolcetti, G.; Marquardt, D. N. *J. Am. Chem. Soc.* **1972**, *94*, 1789−1790. (b) Dumont, W.; Poulin, J. C.; Daud, T. P.; Kagan, H. B. *J. Am. Chem. Soc.* **1973**, *95*, 8295−8299.

(3) Augustine, R. L.; Tanielyan, S. K.; Mahata, N.; Gao, Y.; Zsigmond, A.; Yang, H. *Appl. Catal., A* **2003**, *256*, 69−76.

(4) (a) Special issue on Polyoxometalates in Catalysis , Hill, C. L., Ed.: *J. Mol. Catal. A: Chem.* **2007**, *262*, 1−242. (b) Mizuno, N.; Yamaguchi, K.; Kamata, K. *Coord. Chem. Rev.* **2005**, *249*, 1944−1956. (c) Kholdeeva, O. A. *Top. Catal.* **2006**, *40*, 229−243.

(5) (a) Rong, C.; Pope, M. T. *J. Am. Chem. Soc.* **1992**, *114*, 2932−2938. (b) Lahootun, V.; Besson, C.; Villanneau, R.; Villain, F.; Chamoreau, L. M.; Boubekeur, K.; Blanchard, S.; Thouvenot, R.; Proust, A. *J. Am. Chem. Soc.* **2007**, *129*, 7127−7135. (c) Besson, C.; Chen, S.-W.; Villanneau, R.; Izzet, G.; Proust, A. *Inorg. Chem. Commun.* **2009**, *12*, 1042−1044. (d) Bagno, A.; Bonchio, M.; Sartorel, A.; Scorrano, G. *Eur. J. Inorg. Chem.* **2000**, 17−20. (e) Besson, C.; Geletii, Y. V.; Villain, F.; Villanneau, R.; Hill, C. L.; Proust, A. *Inorg. Chem.* **2009**, *48*, 9436−9443. (f) Besson, C.; Mirebeau, J.-H.; Renaudineau, S.; Roland, S.; Blanchard, S.; Vezin, H.; Courillon, C.; Proust, A. *Inorg. Chem.* **2011**, *50*, 2501−2506. (g) Chen, S.-W.; Villanneau, R.; Li, Y.; Chamoreau, L.-M.; Boubekeur, K.; Thouvenot, R.; Gouzerh, P.; Proust, A. *Eur. J. Inorg. Chem.* **2008**, 2137−2142. (h) Sadakane, M.; Tsukuma, D.; Dickman, M. H.; Bassil, B.; Kortz, U.; Higashijima, M.; Ueda, W. *Dalton Trans* **2006**, 4271−4276. (i) Sadakane, M.; Tsukuma, D.; Dickman, M. H.; Bassil, B.; Kortz, U.; Capron, M.; Ueda, W. *Dalton Trans* **2007**, 2833−2838.

(6) Augustine, R.; Tanielyan, S.; Anderson, S.; Yang, H. *Chem. Commun.* **1999**, 1257.

(7) Kamada, M.; Kominami, H.; Kera, Y. *J. Colloid Interface Sci.* **1996**, *182*, 297−300.

(8) Tarlani, A.; Abedini, M.; Nemati, A.; Khabaz, M.; Amini, M. M. *J. Colloid Interface Sci.* **2006**, *303*, 32−38.

(9) Inumaru, K.; Ishihara, T.; Kamiya, Y.; Okuhara, T.; Yamanaka, S. *Angew. Chem., Int Ed.* **2007**, *46*, 7625−7628.

(10) Liu, H.; Iglesia, E. *J. Phys. Chem. B* **2003**, *107*, 10840−10847.

(11) Li, H.-L.; Perkas, N.; Li, Q.-L.; Gofer, Y.; Koltypin, A.; Gedanken, A. *Langmuir* **2003**, *19*, 10409−10413.

(12) Cheng, L.; Zhu, K.; Bi, L.-H.; Suchopar, A.; Reicke, M.; Mathys, G.; Jaensch, H.; Kortz, U.; Richards, R. M. *Inorg. Chem.* **2007**, *46*, 8457−8459.
(13) Vazylyev, M.; Slobodo-Rozner, D.; Haimov, A.; Mayyan, G.; Neumann, R. *Top. Catal.* **2005**, *34*, 93−99.
(14) Rohlfing, D. F.; Rathousky, J.; Rohlfing, Y.; Bartels, O.; Wark, M. *Langmuir* **2005**, *21*, 11320−11329.
(15) Kato, C. N.; Tanabe, A.; Negishi, S.; Goto, K.; Nomiya, K. *Chem. Lett.* **2005**, *34*, 238−239.
(16) Kasai, J.; Nakagawa, Y.; Uchida, S.; Yamaguchi, K.; Mizuno, N. *Chem.—Eur. J.* **2006**, *12*, 4176−4184.
(17) Mizuno, N.; Kamata, K.; Yamaguchi, K. *Top. Catal.* **2010**, *53*, 876−893.
(18) Kovalchuk, T. V.; Sfihi, H.; Zaitsev, V. N.; Fraissard, J. *Catal. Today* **2011**, *169*, 138−149.
(19) Johnson, B. J. S.; Stein, A. *Inorg. Chem.* **2001**, *40*, 801−808.
(20) Yang, Y.; Guo, Y.; Hu, C.; Wang, E. *Appl. Catal., A* **2004**, *273*, 201−210.
(21) Guo, Y.; Hu, C. *J. Mol. Catal. A: Chem.* **2007**, *262*, 136−148.
(22) Zhou, Y.; Bao, R.; Yue, B.; Gu, M.; Pei, S.; He, H. *J. Mol. Catal. A: Chem.* **2007**, *270*, 50−55.
(23) Schroden, R. C.; Blanford, C. F.; Melde, B. J.; Johnson, B. J. S.; Stein, A. *Chem. Mater.* **2001**, *13*, 1074−1081.
(24) Luo, X.; Yang, C. *Phys. Chem. Chem. Phys.* **2011**, *13*, 7892−7902.
(25) Zhang, R.; Yang, C. *J. Mater. Chem.* **2008**, *18*, 2691−2703.
(26) Tourné, C.; Revel, A.; Tourné, G.; Vendrell, M. *C. R. Acad. Sci., Ser. C* **1973**, *277*, 643−645.
(27) Only one component of this doublet can be viewed, the second being masked by one of the more intense line of the tetrabutylammonium cations. The coupling constant with the phosphorus atom can be only estimated.
(28) Mayer, C. R.; Thouvenot, R. *J. Chem. Soc., Dalton Trans.* **1998**, 7−13.
(29) (a) Villanneau, R.; Racimor, D.; Messner-Henning, E.; Rousselière, H.; Picart, S.; Thouvenot, R.; Proust, A. *Inorg. Chem.* **2011**, *50*, 1164−1166. (b) Villanneau, R.; Ben Djamâa, A.; Chamoreau, L.-M.; Gontard, G.; Proust, A. Submitted.
(30) (a) Kim, G.-S.; Hagen, K. S.; Hill, C. L. *Inorg. Chem.* **1992**, *31*, 5316−5324. (b) Ammari, N.; Hervé, G.; Thouvenot, R. *New J. Chem.* **1991**, *15*, 607−608.
(31) (a) Bareyt, S.; Piligkos, S.; Hasenknopf, B.; Gouzerh, P.; Lacote, E.; Thorimbert, S.; Malacria, M. *Angew. Chem., Int. Ed.* **2003**, *42*, 3404−3406. (b) Bareyt, S.; Piligkos, S.; Hasenknopf, B.; Gouzerh, P.; Lacote, E.; Thorimbert, S.; Malacria, M. *J. Am. Chem. Soc.* **2005**, *127*, 6788−6794.
(32) (a) Xu, B. B.; Wei, Y. G.; Barnes, C. L.; Peng, Z. H. *Angew. Chem., Int. Ed.* **2001**, *40*, 2290−2292. (b) Lu, M.; Wei, Y. G.; Xu, B. B.; Cheung, C. F. C.; Peng, Z. H.; Powell, D. R. *Angew. Chem., Int. Ed.* **2002**, *41*, 1566−1568.
(33) (a) Zhang, J.; Song, Y. F.; Cronin, L.; Liu, T. B. *J. Am. Chem. Soc.* **2008**, *130*, 14408−14409. (b) Zhang, J.; Song, Y. F.; Cronin, L.; Liu, T. B. *Chem.—Eur. J.* **2010**, *16*, 11320−11324.
(34) (a) Odobel, F.; Severac, M.; Pellegrin, Y.; Blart, E.; Fosse, C.; Cannizzo, C.; Mayer, C. R.; Eliott, K. J.; Harriman, A. *Chem.—Eur. J.* **2009**, *15*, 3130−3138. (b) Harriman, A.; Elliott, K. J.; Alamiry, M. A. H.; Le Pleux, L.; Severac, M.; Pellegrin, Y.; Blart, E.; Fosse, C.; Cannizzo, C.; Mayer, C. R.; Odobel, F. *J. Phys. Chem. C* **2009**, *113*, 5834−5842.
(35) (a) Proust, A.; Matt, B.; Villanneau, R.; Guillemot, G.; Gouzerh, P.; Izzet, G. *Chem. Soc. Rev.* **2012**, *41*, 7605−7622. (b) Matt, B.; Coudret, C.; Viala, C.; Jouvenot, D.; Loiseau, F.; Izzet, G.; Proust, A. *Inorg. Chem.* **2011**, *50*, 7761−7768. (c) Matt, B.; Renaudineau, S.; Chamoreau, L.-M.; Afonso, C.; Izzet, G.; Proust, A. *J. Org. Chem.* **2011**, *76*, 3107−3112. (d) Matt, B.; Moussa, J.; Chamoreau, L.-M.; Afonso, C.; Proust, A.; Amouri, H.; Izzet, G. *Organometallics* **2012**, *31*, 35−38.
(36) Mercier, D.; Boujday, S.; Annabi, C.; Villanneau, R.; Pradier, C.-M.; Proust, A. *J. Phys. Chem. C* **2012**, *116*, 13217−13224.
(37) (a) Hoffmann, F.; Cornelius, M.; Morell, J.; Froeba, M. *Angew. Chem., Int. Ed.* **2006**, *45*, 3216−3251. (b) Zeleňák, V.; Badaničová, M.; Halamová, D.; Čejka, J.; Zukal, A.; Murafa, N.; Goerigk, G. *Chem. Eng. J.* **2008**, *144* (15), 336−342.
(38) (a) Karimi, Z.; Mahjoub, A. R.; Davari Aghdam, F. *Inorg. Chim. Acta* **2009**, *362*, 3725−3730. (b) Jin, H.; Wu, Q.; Zhang, P.; Pang, W. *Solid State Sci.* **2005**, *7*, 333−337. (c) Bae, J. A.; Song, K.-C.; Jeon, J.-K.; Soo, Ko, Y. *Microporous Mesoporous Mater.* **2009**, *123*, 289−297.
(39) Lapisardi, G.; Chiker, F.; Launay, F.; Nogier, J. P.; Bonardet, J. L. *Appl. Catal., A* **2003**, *243*, 309−321.
(40) Kharat, A. N.; Moosavikia, S.; Jahromi, B. T.; Badiei, A. *J. Mol. Catal. A: Chem.* **2011**, *348*, 14−19.
(41) (a) Espinosa, M.; Pacheco, S.; Rodriguez, R. *J. Non-Cryst. Solids* **2007**, *353*, 2573−2581. (b) Abdullah, A. Z.; Salamatinia, B.; Kamaruddin, A. H. *Biochem. Eng. J.* **2009**, *44*, 263−270.
(42) (a) Hu, J.; Li, K.; Li, W.; Ma, F.; Guo, Y. *Appl. Catal., A* **2009**, *364*, 211−220. (b) Rao, P. M.; Wolfson, A.; Kababya, S.; Vega, S.; Landau, M. V. *J. Catal.* **2005**, *232*, 210−225. (c) Kim, H.; Jung, J. C.; Yeom, S. H.; Lee, K.-Y.; Yi, J.; Song, I. K. *Mater. Res. Bull.* **2007**, *42*, 2132−2142. (d) Rao, P. M.; Landau, M. V.; Wolfson, A.; Shapira-Tchelet, A. M.; Herskowitz, M. *Microporous Mesoporous Mater.* **2005**, *80*, 43−55.
(43) The signal is strongly displaced due to the presence of a large amount of triethylamine, which role is to deprotonate the carboxylic acid functions.